

Automatic Detection of Traffic Infrastructure Objects for the Rapid Generation of Detailed Digital Maps using Laser Scanners

Thorsten Weiss and Klaus Dietmayer

Abstract—Detailed digital maps are of benefit for navigation systems and also for future driver assistant and safety applications. The generation of detailed digital maps is an expensive and time-consuming process as there is much manual rework. In this work, algorithms for the automatic detection of traffic infrastructure objects are proposed. The accurate positions of lane markings, sidewalks, reflection posts and guardrails are determined automatically by a vertically and a horizontally mounted automotive laser scanner. The high position accuracy of the mapped traffic infrastructure objects allows for the rapid generation of up to date, accurate and detailed digital infrastructure maps with a cost efficient sensor setup and a low demand for manual rework.

I. INTRODUCTION

A detailed environmental description containing stationary traffic infrastructure objects provides important information for future intelligent vehicles and future advanced driver assistant systems. Today's digital maps contain various traffic infrastructure objects, such as the position and the number of lanes, intersections and also points of interest. The position accuracy of the objects in these maps is sufficient for navigation purposes. However, the generation of these navigation maps is an expensive and time-consuming process as the data collected by surveillance vehicles, air photographs or surveillance departments has to be reworked manually.

Furthermore, a more detailed representation of the traffic infrastructure is of benefit for common and more precise navigation systems. Future driver assistant systems also benefit from detailed maps as shown in the EC-project INTERSAFE, for instance [1]. In this project a precise host localization approach and detailed digital maps helped to improve tracking and classification algorithms and enabled new intersection safety applications [1], [2], [3], [4].

In order to support the generation of these maps, algorithms for the automatic detection and mapping of traffic infrastructure objects are proposed. For the mapping process two automotive laser scanners are used to detect the traffic infrastructure objects. One laser scanner is mounted at the front bumper of the mapping vehicle, providing horizontal distance profiles for the automatic mapping of reflexion posts, barriers, house walls and the semiautomatic mapping of posts of traffic lights and signs. The second one is mounted on the back of the vehicle providing vertical distance profiles for the automatic detection and position determination of lane

markings, guardrails, crash barriers and curbs of sidewalks. The detection algorithms are described in section IV to V.

In order to register the TIOs¹ relative to a global digital map, the position of the vehicle must also be known relative to a global coordinate system. Therefore, a RTK-GPS receiver or a low-cost DGPS receiver is used. Algorithms for the determination of the trajectory of the mapping vehicle are introduced in section III. Quantitative Analysis using a ground truth reference system are added to each section.



Fig. 1. *Left:* Horizontally mounted ALASCA XT laser scanner. *Right:* Vertically mounted ALASCA XT laser scanner.

II. SENSOR SETUP

The multilayer laser scanner ALASCA XT (Automotive LaserScanner) of the company IBEO Automobile Sensor GmbH acquires distance profiles of up to 240° horizontal field of view. The scan frequency is chosen to 10 Hz in this work. The range resolution is 4 cm and the angle resolution is chosen to 0.25°. The laser scanners have four individual scan planes with a vertical opening angle of 3.2°. The laser scanners are integrated in a rugged enclosure and they are calibrated and synchronized. One laser scanner is mounted vertically above the roof on the back of the vehicle. Another laser scanner is mounted on the front bumper as shown in Fig. 1.

III. TRAJECTORY DETERMINATION

A. Coordinate systems

The sensors provide the positions of detected TIOs in their own sensor coordinate system ζ^{LS} . As the sensors are calibrated, the detected objects are transformed to the vehicle's coordinate system ζ^{veh} .

The detected infrastructure objects are registered in world coordinates. In this approach the geographic coordinate system WGS-84 (ζ^{WGS84}) is used. There are two reasons for

¹TIO - traffic infrastructure object

Thorsten Weiss is with at the Department Measurement, Control and Microtechnology, University of Ulm, D-89081 Ulm, Germany, PhD, thorsten.weiss@uni-ulm.de

Klaus Dietmayer is professor at the Department Measurement, Control and Microtechnology, klaus.dietmayer@uni-ulm.de

choosing this system. Firstly, most GPS receivers provide their position measurements in WGS-84 coordinates and secondly, many map databases also use this system [5].

The TIOs are transformed to the WGS-84 coordinate system in the following steps. Firstly, the coordinates are transformed to a local tangent plane coordinate system ζ^{TP} and then to the ECEF-coordinate ζ^{ECEF} system and finally to the WGS-84 coordinate system ζ^{WGS84} as described in detail in [2], [6]. The entire transformation is then:

$$\zeta^{Sensor} \rightarrow \zeta^{vehicle} \rightarrow \zeta^{TP} \rightarrow \zeta^{ECEF} \rightarrow \zeta^{WGS84} \quad (1)$$

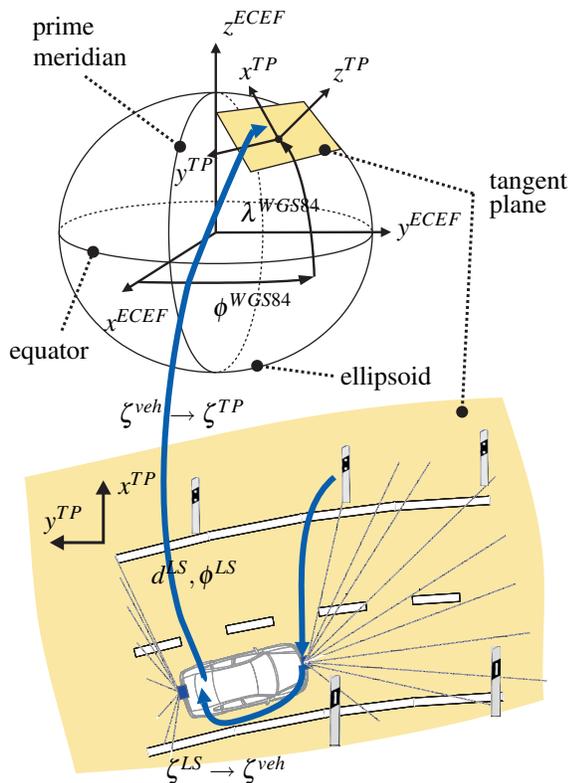


Fig. 2. Coordinate Transformation of TIOs.

B. GPS receivers

The pose² of the mapping vehicle must be known precisely for each point of time laser scans are captured.

In this work the position is determined using different types of GPS receivers. However, the position accuracy of standard GPS receivers is in the range of 5-20 m depending on the environment and the performance of the receiver. Consequently, the position accuracy in world coordinates of the detected objects will be poor, if a standard GPS receiver is used.

For this reason, two types of differential GPS receivers are used. The Novatel DL-4 plus RTK-GPS³ receiver provides position measurements at an accuracy of 3 cm in optimal

conditions. The update rate is 10 Hz. The RTK-GPS receiver and the laser scanners are synchronized. In urban areas, street canyons or other suboptimal regions, where RTK-GPS will not provide this high position accuracy, an IMU⁴ determines the pose precisely even in these hard conditions.

A low-cost solution is a DGPS⁵ receiver such as the Afusoft Raven 6 using differential data from RASANT⁶ or EGNOS⁷. The position accuracy of these receivers is in the magnitude of about 3 m [7]. However, the relative position between the position measurements of the DGPS receiver is in the 10 cm level. This leads to a consistent and accurate map concerning the relative positions of the TIOs, but with an offset error of up to 3 m. If a low cost mapping systems is required, the system still provides accurate maps with much information. In the following section an algorithm is introduced, which enables the determination of the pose of the vehicle from both DGPS and RTK-GPS position measurements.

C. Temporal interpolation

DGPS provides one position measurement per second. The laser scanners provide 10 distance profiles per second. Consequently, the pose of the vehicle between two GPS measurements is not known. In order to determine the pose of the vehicle for arbitrary update rates of GPS systems, an algorithm for the interpolation of GPS position measurements was developed. A GPS receiver is not able to measure the orientation of the mapping vehicle directly, as it only measures positions. Therefore, the interpolation algorithm must also determine the correct orientation of the vehicle. The interpolation algorithm must satisfy several criteria in order to generate consistent maps:

- There must not be any jumps or jitters in the trajectory, as this would lead to an inconsistent map and also jumps in the map, respectively.
- Acceleration and deceleration of the mapping vehicle must be considered for, even for 1 Hz data.
- The algorithm must be able to deal with different update rates of the GPS receivers.
- The algorithm must be able to handle any form of trajectory.

A spatial interpolation of the position measurements by simply fitting a spline to the position measurements will not fulfill these requirements, because acceleration and deceleration will not be modeled. If a trajectory is crossing itself during a mapping process, a simple spline interpolation will not be able to represent a valid trajectory due to ambiguities.

In order to solve these problems, the coordinates are not interpolated spatially, but they are interpolated temporally. For this purpose, the coordinates are interpolated separately as a function of time as shown in Fig. 3 and Fig. 4.

In a next step a spline is fitted to these points. The times laser scans are captured are selected in the plots.

⁴IMU - Inertial Measurement Unit

⁵DGPS - Differential Global Positioning System

⁶RASANT - Radio Aided Satellite Navigation Technique

⁷EGNOS - European Geostationary Navigation Overlay Service

²pose - position and orientation

³RTK- Real Time Kinematik

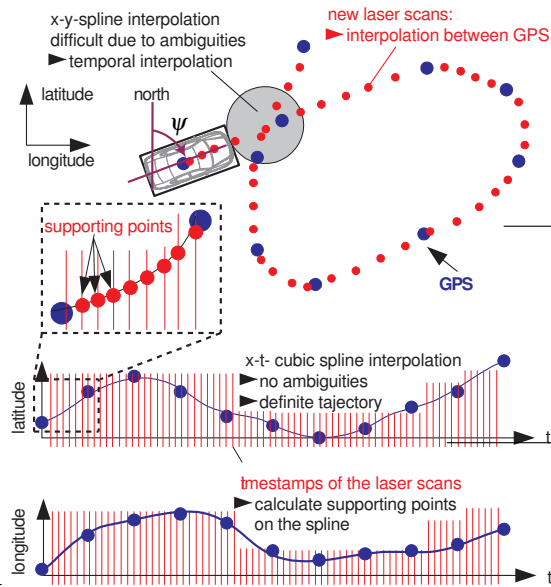


Fig. 3. In order to provide a consistent trajectory between the GPS measurements, a temporal interpolation based on cubic splines is applied.

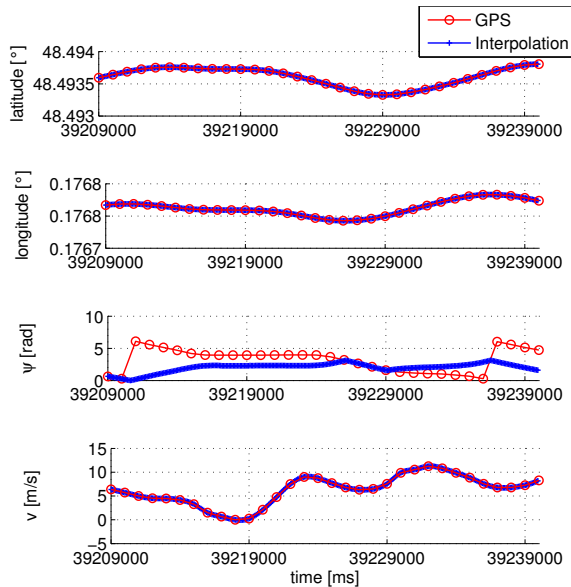


Fig. 4. The coordinates are interpolated separately. The trajectory is shown in Fig. 5.

By calculating supporting points on the spline, the position of the mapping vehicle can be determined for any time. Consequently, the algorithm allows for the determination of a trajectory for varying update rates of the GPS and the laser scanner. Furthermore, information about the acceleration and deceleration of the mapping vehicle is given by the slope of the interpolated curves.

The orientation of the vehicle is calculated from the splines in the supporting points. The orientation of the vehicle is the angle between the longitudinal axis of the vehicle and

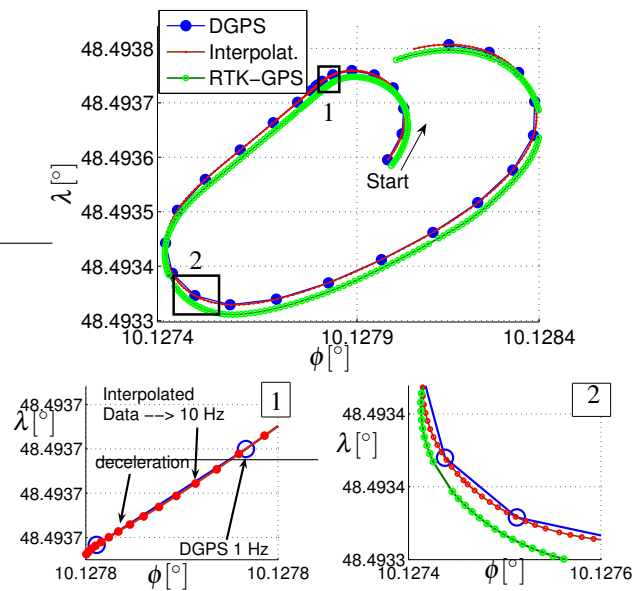


Fig. 5. Resulting trajectory of the temporal interpolation in Fig. 4. As can be seen in the cut-out **1** the deceleration of the vehicle is represented correctly even for 1 Hz DGPS data. The green line shows the RTK-GPS reference measurements. The shape of the trajectory provided by DGPS is very similar to the accurate RTK-GPS trajectory, but with an offset error. This could be observed in extensive tests in different scenarios.

geographic north. Given the spline polynomial of between two GPS points $\lambda_{spl}(t)$ (latitude) and $\phi_{spl}(t)$ (longitude), the orientation $\psi(t)$ of the vehicle is (see Fig. 3):

$$\psi(t) = \frac{\frac{\partial \lambda_{spl}(t)}{\partial t}}{\frac{\partial \phi_{spl}(t)}{\partial t}} = \frac{\partial \lambda_{spl}(t)}{\partial \phi_{spl}(t)} \quad (2)$$

The interpolation works for all trajectories as there are no ambiguities in the curve progression (see Fig. 3).

Fig. 4 and 5 shows the results of an exemplary test drive. Extensive tests in different scenarios have shown similar results.

Reference measurements using RTK-GPS of the interpolated DGPS trajectory has shown that the relative position error of DGPS is in the range of **< 10 cm** for neighboring points at a speed of up to 60 km/h, if there are no abrupt curve maneuvers.

IV. AUTOMATIC MAPPING OF GUARDRAILS AND SIDEWALKS

Guardrails and curbs of sidewalks are detected robustly and mapped automatically using the vertically mounted laser scanner. The algorithm is subdivided into several modules, which are shown in Fig. 6.

A. Gaussian filter

A third-order gaussian filter is applied in order to sharpen the vertical distance profile. Fig. 7 shows the raw and the filtered distance profile.

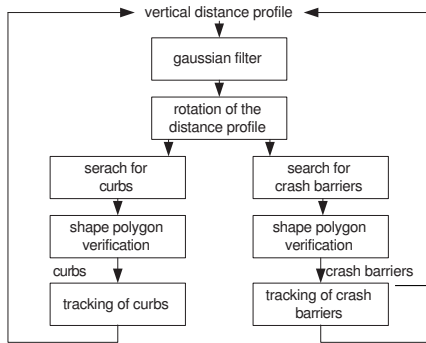


Fig. 6. Algorithm for the detection and tracking of guardrails and curbs (sidewalks and small walls)

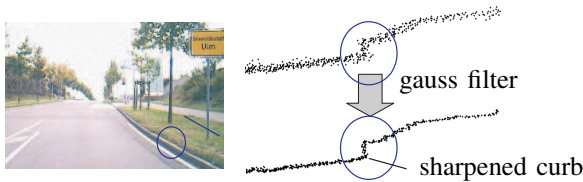


Fig. 7. The gaussian filter sharpens the shape of the curb. The video reference image shows the curb.

B. Rotation of the distance profile

The distance profile is rotated in order to align the distance profile parallel to the road for the compensation of vehicle rolling. Therefore, a regression line is fitted to the middle of the vertical distance profile. The distance profile is rotated.

C. Search for curb and guardrail candidates using histograms

In order to find candidates for curbs and guardrails a histogram based algorithm is used. Therefore, the distance profile is subdivided into sections with a certain width (20 cm) and the scan points, which are inside the sections are accumulated. As the angular resolution of the laser scanner is 0.25° the number of potential scan points per section is greater for sections near $y^{LS} = 0$ than for sections with a larger lateral distance. Therefore, the number of points in each histogram slot is multiplied by a correction factor. Regarding the geometric constellation a linear equation was determined:

$$C_{hi}(y_{hi}^{LS}) = 0.06 + 0,03 \frac{1}{m} \cdot |y_{hi}^{LS}| \quad (3)$$

where y_{hi}^{LS} is the middle position of the i -th histogram slot and C_{hi} is the correction factor for the i -th slot. Curbs are situated near the road. That's why curbs are only searched for in a certain height over the road

$$x_{min,curb}^{LS} < x_{curb}^{LS} < x_{max,curb}^{LS} \quad (4)$$

where $x_{min,curb}^{LS}$ is the minimum height relative to the road surface and $x_{max,curb}^{LS}$ is the maximum height. Guardrails are

situated at a specific height over the road. Consequently, the search area for guard rails can also be reduced to

$$x_{min,cb}^{LS} < x_{cb}^{LS} < x_{max,cb}^{LS} \quad (5)$$

as shown in Fig. 8.

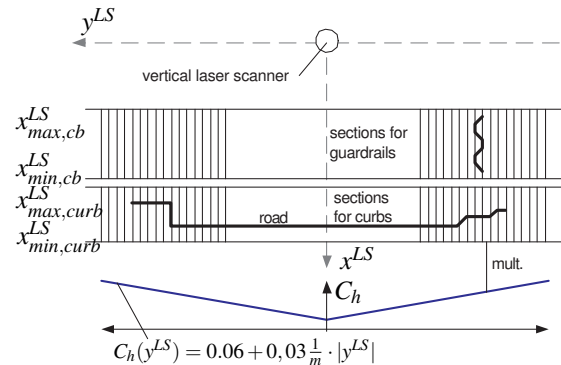


Fig. 8. Distance measurements are accumulated in two histograms, one for guardrails and one for curbs for different heights over the road surface.

D. Shape polygon

The previously introduced histogram algorithm provides candidates for curbs and guardrails. However, not every candidate is a valid guardrail or curb. That's why a verification algorithm is applied. A shape polygon is fitted to the points in the region of a histogram peak. The polygon represents the shape of the measurement points. If the design parameter R is chosen small, fine nuances of the shapes are represented by the polygon. For larger R values, the shapes are smoothed. With the help of this polygon, some features are calculated. For curbs, the height and the slope of the shape are strong features. Furthermore, a curb-polygon must not be interrupted. Regarding these three features, the polygon is classified as a curb or it is neglected (see Fig. 10).

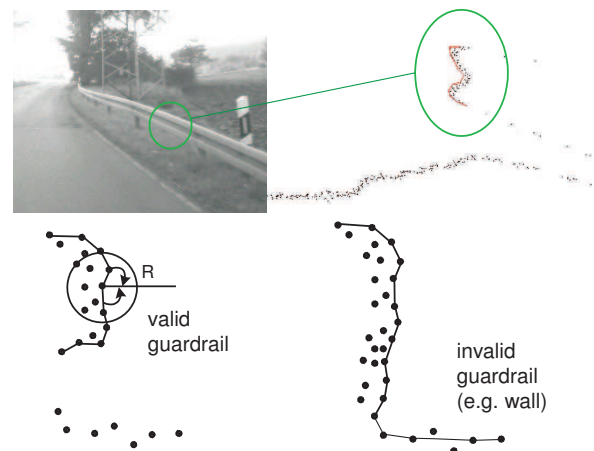


Fig. 9. The upper image shows the shape of a guardrail in a laser scan. The lower part shows a valid and an invalid guardrail. Equivalent to the curb verification the design parameter R is applied here.

Also for guardrails unique features can be found. The shape can be found at a specific height over the road and

has a typical "lying U-shape" as shown in Fig. 9. Furthermore, the dimension of the polygon provides a feature for guardrails. Regarding these features, the polygon is classified as a guardrail or it is neglected. Fig. 10 shows some examples for valid and invalid polygons.

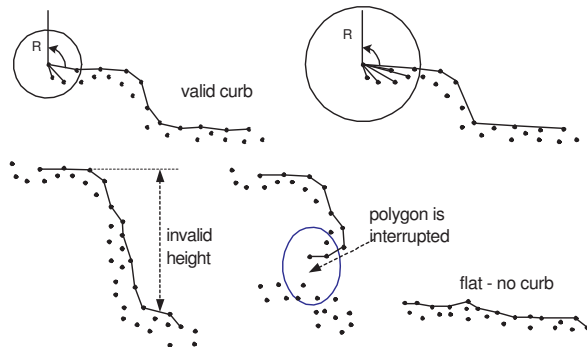


Fig. 10. The upper two images illustrate the effect of the design parameter R for the shape polygon for curbs. In Fig. 7 a measured distance profile of a curb is illustrated. Three examples of invalid curbs are shown in the lower part of the image. The histogram may have provided these point sets as a candidate. The shape polygon excludes these invalid detections.

E. Tracking

In order to provide a continuous guardrail- and curb object, these objects are tracked using a multi object tracking based on Kalman Filters. The tracking algorithm estimates the lateral position of the objects. Invalid detections can be excluded and the detections in each scan are associated.

F. Quantitative analysis

In order to analyze the position accuracy of the mapped objects, an RTK-GPS receiver is used. In static mode, the RTK-GPS receiver is able to measure positions at an accuracy of <1 cm, if the receiver antenna remains at a position for several minutes. The curbs were passed by the mapping vehicle at different speeds (>30 - 50 km/h). The positions of the detected curbs are compared to the positions from the accurate RTK-GPS static mode measurements. The pose of the vehicle during the mapping process was determined using RTK-GPS in dynamic mode. The accuracy in dynamic mode is lower. Fig. 11 shows the absolute position error of an exemplary test drive. The results for different types and heights of curbs are in the same region. The position accuracy of TOIs depends on the accuracy of the positioning system, respectively. By using DGPS, the relative position accuracy is in the same region, but with lower absolute position accuracy.

The positions of some guardrails were also measured and compared to the positions of detected and tracked objects. Fig. 12 shows an automatically mapped guardrail and the absolute position error.

Furthermore, the reliability of the curb and guardrail mapping algorithms was analyzed. Therefore, a test set of scans containing several curbs and guardrails were labeled. There were also scans without any curbs or guardrails. The detection rate for curbs is about 90% within the tested scenarios for not occluded curbs in the field of view of

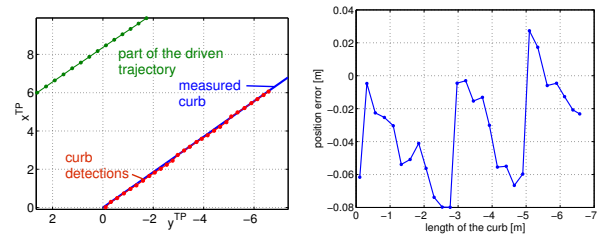


Fig. 11. The green line is a part of the driven trajectory of the mapping vehicle. The blue line represents the ground truth position of the curb measured by RTK-GPS in static mode. The red line shows the positions of the detected and tracked curb in the map. For better visualization, the geographic coordinates were transformed to a tangent plane coordinate system.

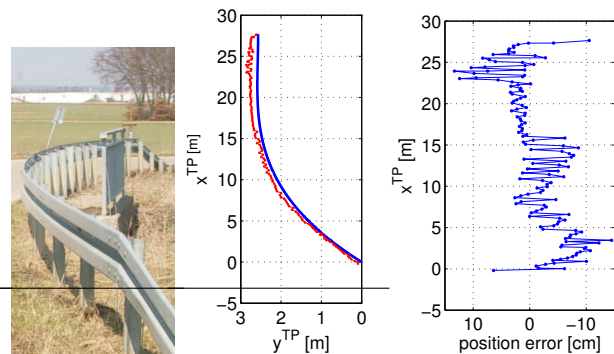


Fig. 12. The blue line represents the guardrail's position measured by RTK-GPS in static mode. The red line is the position of the detected and tracked guardrail in the map.

the vertically mounted laser scanner. The detection rate for guardrails is about 85% without tracking.

V. MAPPING OF LANE MARKINGS

Modern navigation maps contain the number of lanes and the curvature of road elements. In this work algorithms for the detection and mapping of traffic markings using the vertically mounted laser scanner are proposed. This enables the determination of the width and the position of lanes accurately. Detected lane markings are registered in a digital map automatically.

A. Detection of lane markings

The laser scanners analyze the EPW⁸ of each laser beam. The EPW is a measurement for the reflectivity of a detected object. In this approach the EPW is used to separate tarmac and the well reflecting traffic markings. Fig. 13 shows a typical vertical scan and the EPW of the laser beams.

1) *Peak Extraction:* Peaks in the EPW curve represent reflecting objects. Beyond traffic markings, reflecting objects such as grass on the roadside show also peaks in the EPW. In order to register only traffic markings in the digital map, peaks representing traffic markings are determined.

However, the traffic markings are made of different materials with different reflection characteristics. In Germany, for

⁸EPW - echo pulse width

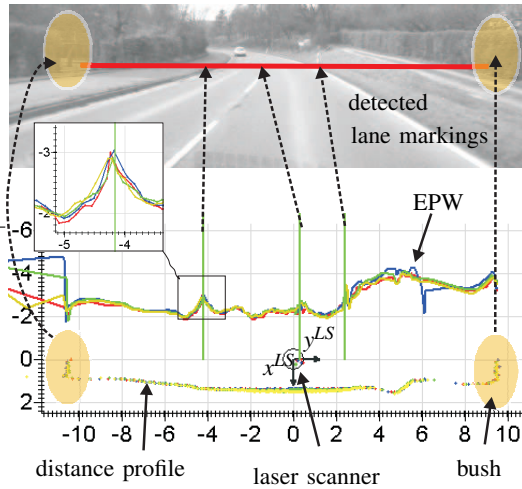


Fig. 13. Smoothed EPW of the vertically mounted laser scanner. The peaks represent traffic markings.

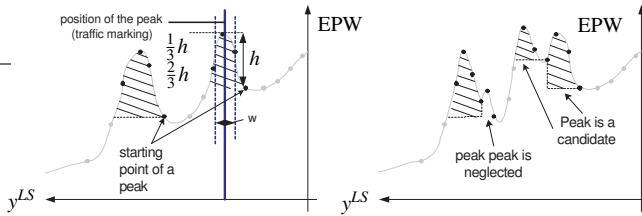


Fig. 14. Illustration of the peak extraction. The position of peaks is determined as shown in the left image. The right image shows two neglected peaks.

instance, mostly three types of materials for traffic markings are used [8]. Furthermore, the width of traffic markings may be different.

Extensive tests with different materials for traffic markings have shown, that there are some common features. The width and the height of the peaks as well as the gradient of the peaks are strong features for the traffic markings. Furthermore the traffic markings can not be situated above the road. The algorithm described here determines these four features for every peak candidate.

- First of all, a one dimensional Gaussian Filter is applied to the EPW in order to smooth the curve.
- Beginning from the middle of the scan ($y_{LS} = 0$ m) the difference of adjacent smoothed points are calculated. If the difference falls above a parameter d_{EPW} the difference between the starting point and the maximum of the slope is calculated. (Parameter h in Fig. 14)
- If the curve falls below its starting point, the height h and the width w of the peak are calculated. The height of the peak must be greater than h_{min} . The width must be in the range of w_{min} and w_{max} . The peak must be situated near the road (y_{peak}^{LS}). The peak is classified as a candidate TM_{true} , otherwise the peak is neglected:

$$TM_{true} = (h \geq h_{min}) \cap (w_{min} \leq w_{peak} \leq w_{max}) \cap (y_{min}^{LS} \leq y_{peak}^{LS} \leq y_{max}^{LS}) \quad (6)$$

- The x^{LS} -coordinate of the center of the peak is calculated as shown in figure 14.
- As there are four scan layers the peak extraction is performed for each layer separately and valid candidates are combined.

2) *Tracking*: After the peak extraction step the lane candidates are tracked. This allows excluding outliers and invalid traffic markings as well as the detection of dashed traffic markings (see section IV-E). Fig. 15 shows an example of a tracked line.

B. Quantitive analysis

The approach works reliable at a high detection rate for lateral distances up to ± 5 m. For distances up to 15 m also peaks are detected, but with lower detection rate, as the number of scan points on the ground gets less for greater lateral positions.

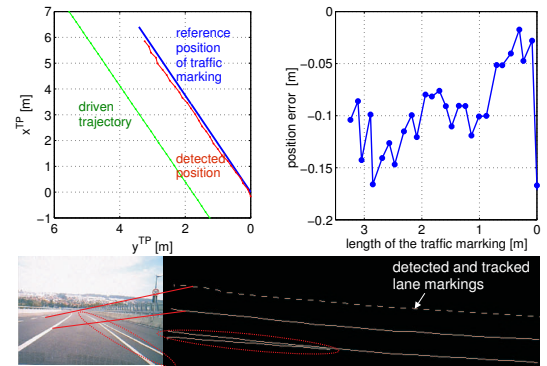


Fig. 15. Driven trajectory, ground truth position of the traffic marking and the position of the detected marking. The lower image shows an exemplary automatically mapped traffic marking. Dashed lines and drawn through lines are separated using the tracking system.

The analysis concerning the position accuracy were performed analogous to the analysis of the curbs and guardrails. The positions of different traffic markings were measured by RTK-GPS and compared to the detected position. Results are shown in Fig. 15.

VI. MAPPING OF REFLEXION POSTS

A. Detection of reflexion posts

In this work the detection and the automatic mapping of reflexion posts using the horizontally mounted laser scanner is introduced. Reflexion posts are equipped with retro reflectors [8], which are detected by analyzing the EPW. Another feature for the detection of reflexion posts are the size of the posts. Another less strong feature is the pairwise arrangement of the reflexion posts.

In the first step, candidates in the actual distance profile are searched for. The laser scan is clustered to segments. Small

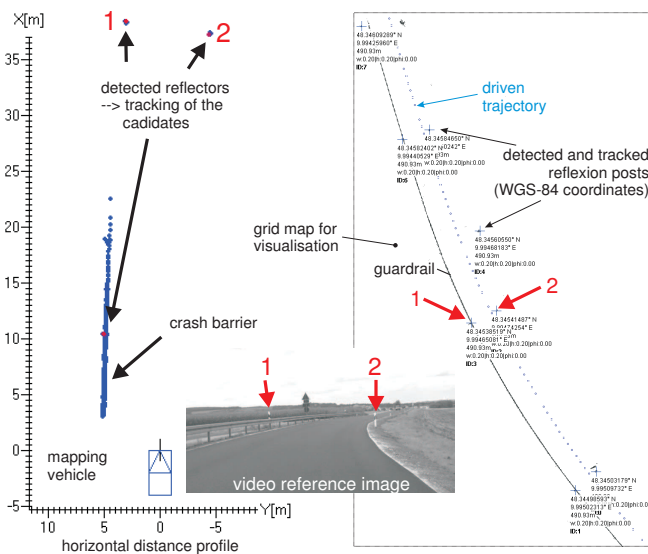


Fig. 16. Distance Profile of a horizontally mounted laser scanner. Detected reflectors are painted red. The posts were detected, tracked and registered in a map. For a better visualization of the scene, the grid map (accumulated laser scans) is shown in the right image, which shows the WGS-84 coordinates of the automatically mapped reflexion posts. The video reference image shows the scenario.

segments and segments containing distance measurements with reflectors are candidates. The small objects are tracked using a multi object Kalman Filter. After the mapping vehicle passed a reflexion post the number of scans, where a reflector was detected in the small objects, is analyzed. The arrangement of the objects is analyzed. The approach is optimized for the mapping of reflexion posts on highways and country roads. Fig. 16 shows an example.

B. Quantitative analysis

The position of a reflexion post was measured using RTK-GPS. The mapping vehicle passed the post at different distances and different velocities (20 km/h-50 km/h). Six exemplary results are given here. The speed of the mapping vehicle is about 20 km/h for drive 1 up to about 50 km/h for drive 5. The post was passed in a lateral distance of about 1 m-3 m and a lateral distance of about 10 m - 20 m. There were no abrupt curve maneuvers during the mapping process. The absolute position error of the mapped reflexion post in centimeters is given in the following table:

drive		1	2	3	4	5	6
pos.err [cm] (1m - 3m)		6,23	9,5	12,1	23,4	13,6	11,8
pos.err [cm] (10m - 20m)		8,17	14,4	17,7	21,1	14,4	15,3

VII. CONCLUSIONS AND FUTURE WORK

The main focus of this work is the detection of traffic infrastructure objects using laser scanners in order to support the generation of cost-effective and up to date digital maps. The high position accuracy of the detected objects could be shown using a reference system. In future works a video system could be used to detect more traffic infrastructure objects, such as traffic signs or also reflexion posts [9], [10]. Furthermore image processing could improve

the detection of traffic markings, especially for the detection of arrows or other special forms of traffic markings.

VIII. ACKNOWLEDGEMENTS

This work is supported by IBEO Automobile Sensor GmbH (www.ibeo-as.de). Further information is available on www.argos.uni-ulm.de

REFERENCES

- [1] K. C. Fuerstenberg and U. Lages, "New european approach for intersection safety the ec-project intersafe," *Proceedings of IEEE Intelligent Vehicles Symposium 2005, Las Vegas, USA*, 2005.
- [2] T. Weiss, N. Kaempchen, and K. Dietmayer, "Precise ego-localization in urban areas using laserscanner and high accuracy feature maps," *Proceedings of IEEE Intelligent Vehicles Symposium 2005, Las Vegas, USA*, 2005.
- [3] S. Wender, T. Weiss, and K. Dietmayer, "Improved object classification of laserscanner measurements at intersections using precise high level maps," *Proceedings of the 8th International IEEE Conference on Intelligent Transportation Systems, Vienna, Austria*, 2005.
- [4] K. Frstenberg, J. Chen, and S. Deuschle, "New european approach for intersection safety results of the ec-project intersafe," in *WIT 2007, 4th International Workshop on Intelligent Transportation*, 2007.
- [5] O. G. C. Inc., "Opengis specifications," Website, 2006. [Online]. Available: <http://www.opengeospatial.org/standards>
- [6] J. Farrell, T. Givargis, and M. Barth, *Real-Time Differential CarrierPhase GPS-Aided INS*. IEEE Transaction on Control Systems Technology Vol.8, July 2000.
- [7] AFUSOFT. www.afusoft.com, 2006.
- [8] E. Knoll, *Der Elsner - Handbuch fuer Strassen- und Verkehrswesen - Handbook for roads and transportation*. Otto Elsner Verlagsgesellschaft, 2004.
- [9] D. M. Gavrilu, "Traffic sign recognition revisited," in *DAGM-Symposium*, 1999, pp. 86-93. [Online]. Available: citeseer.ist.psu.edu/gavrilu99traffic.html
- [10] M. S. von Trzebiatowski, A. Gern, U. Franke, U.-P. Kaeppler, and P. Levi, "Detecting reflection posts - lane recognition on country roads," in *2004 IEEE Intelligent Vehicles Symposium, University of Parma, Parma, Italy*, 2004.